



## Regular Article

# High Shear Dependent von Willebrand Factor Self-assembly Fostered by Platelet Interaction and Controlled by ADAMTS13



Thorsten Kragh <sup>a,\*</sup>, Marina Napoleone <sup>a</sup>, Mohammad A. Fallah <sup>b</sup>, Herbert Gritsch <sup>c</sup>,  
Matthias F. Schneider <sup>d</sup>, Armin J. Reininger <sup>c</sup>

<sup>a</sup> Department of Transfusion Medicine, Cell Therapeutics and Hemostasis, Medical Center of the University of Munich, Germany

<sup>b</sup> Department of Biophysical Chemistry, University of Konstanz, Germany

<sup>c</sup> Baxter Innovations GmbH, Vienna, Austria

<sup>d</sup> Boston University, Department of Mechanical Engineering, Boston, MA, USA

## ARTICLE INFO

## Article history:

Received 25 September 2013

Received in revised form 6 February 2014

Accepted 3 March 2014

Available online 10 March 2014

## Keywords:

Ultralarge von Willebrand factor

Fluid high shear

Wall parallel flow

Stagnation point flow

ADAMTS 13

VWF-platelet conglomerates

## ABSTRACT

**Introduction:** The paradigm of activation induced platelet aggregation has recently been refuted under blood flow conditions with shear rates exceeding  $20,000\text{ s}^{-1}$ . These lead to reversible rolling platelet aggregates, which were dependent on the presence of immobilized and soluble von Willebrand factor.

**Material and Methods:** In vitro experiments using direct fluorescence video-microscopy were performed in wall parallel and stagnation point flow chambers with shear rates raised from  $20,000$  to  $50,000\text{ s}^{-1}$ . Washed blood cell suspension containing recombinant von Willebrand factor (rVWF) was perfused over rVWF or collagen coated surfaces.

**Results:** Here we show for the first time with the visualization of rVWF that not only colloid and polymer, i.e. platelets and VWF, form a composite, but that VWF itself is capable of entirely reversible self-assembly. On a collagen surface the platelet-VWF-conglomerates did not roll but VWF nets bound permanently to the collagen fibers and captured and immobilized platelets from the flow. Lowering the shear rate below the threshold of  $20,000\text{ s}^{-1}$  no longer dissolved these deposits. Ultralarge multimer containing rVWF was most effective compared to normal sized rVWF. The presence of ADAMTS13 limited rolling aggregate and platelet-VWF-conglomerate formation to a time window of 7–8 minutes. Changing wall parallel flow to stagnation point flow halved the required shear rate threshold.

**Conclusion:** We conclude that flow dynamics can trigger reversible von Willebrand factor self-assembly and platelet-VWF-conglomerate accrual, which are regulated by ADAMTS13 to a time span needed by coagulation to stabilize it, e.g. in case of vessel injury.

© 2014 Elsevier Ltd. All rights reserved.

## Introduction

Platelet accrual at sites of vascular injury requires arrest of non-activated platelets from fast flowing blood, succeeded by their activation and stabilization as an aggregate and ultimately a thrombus. The initial step is thought to be single platelet adhesion to immobilized von Willebrand factor via their GPIIb/IIIa receptor. However in the case of a vessel leak this platelet accumulation – one at a time – may not suffice for efficient stop of bleeding. In addition vessel leaks or stenosis may exhibit flow conditions with excessively elevated shear rates that appear

to counteract cellular deposition. Ruggeri and coworkers have put forward a mechanism of rolling platelet aggregate formation independent of platelet activation and signaling. The process was entirely reversible if the shear rate fell below a critical threshold of  $20,000\text{ s}^{-1}$  [1]. We recently applied it to blood-clotting-inspired reversible polymer-colloid composite assembly in flow [2]. There model simulations were used to show the flow-driven self-assembly between polymer and colloid, i.e. VWF and platelet. Interestingly, the propensity to form such composites is in contrast to our intuitive expectation, where laminar shear flow conditions may rather be expected to decrease association. Thus the clotting scenario in which flow controls the reversible assembly of complex composites was described to represent a completely new aggregation paradigm in blood flow that cannot be understood in terms of purely diffusion-limited and/or reaction-limited aggregation concepts [2]. The examined shear rates were up to  $14,000\text{ s}^{-1}$  and the corresponding VWF GPIIb/IIIa-bond breakup force was estimated to be in the order of  $\sim 10\text{ pN}$ . In the present paper we have taken this a step further and examined the influence of two different flow conditions -wall parallel

**Abbreviations:** BSA, bovin serum albumin; EDTA, ethylenediaminetetraacetic acid; GPIIb/IIIa, glycoprotein IIb/IIIa; PBS, phosphate buffered saline; PGE1, prostaglandin E1; PPACK, H-D-Phe-Pro-Arg-chloromethylketone trifluoroacetate salt; rADAMTS13, a recombinant disintegrin and metalloproteinase with a thrombospondin type 1 motif, member 13; rVWF, recombinant von Willebrand factor; UL, ultra large.

\* Corresponding author at: Max-Lebsche-Platz 32, 81377 Munich, Germany. Tel.: +49 89 70954412; fax: +49 89 70954416.

E-mail address: [thorsten.kragh@med.uni-muenchen.de](mailto:thorsten.kragh@med.uni-muenchen.de) (T. Kragh).

and stagnation point flow- on the self-assembly of the VWF polymer in solution and on the surface while increasing the shear rates up to  $50,000 \text{ s}^{-1}$  and introducing the cleaving enzyme ADAMTS 13. In addition we examined the effect of a fibrillar collagen surface and the size distribution of the VWF multimers.

## Material and Methods

All procedures involving human subjects were conducted in accordance with the Declaration of Helsinki and were approved by the Ethics Commission of the Ludwig-Maximilians-University Munich. Informed consent was obtained from all participating subjects.

### Fluid Preparation for Flow Experiments

Blood sample collection and preparation was performed as previously described [1]. For perfusion studies, blood from healthy human volunteers was drawn from an antecubital vein and collected into S-Monovettes (Sarstedt AG&Co, Nümbrecht, Germany) containing the disodium salt of ethylenediamine tetraacetic acid (EDTA, 1.6 mg/ml blood; Sarstedt). H-D-Phe-Pro-Arg-chloromethylketone trifluoroacetate salt (PPACK, final concentration  $46 \mu\text{M}$ ; Bachem Bioscience, King of Prussia, PA), prostaglandin (PG)  $\text{E}_1$  (final concentration  $14 \mu\text{M}$ ; Sigma-Aldrich Chemie, Taufkirchen), and apyrase from potato (Grade 3, 1.3 ATPase U/ml blood; Sigma-Aldrich Chemie) were added to the blood when indicated to inhibit platelet activation and block integrin function.

For washed cell suspensions the blood was centrifuged at  $1400 \text{ g}$  for 13 min at room temperature ( $22^\circ\text{C} - 25^\circ\text{C}$ ). The supernatant plasma was discarded and the platelets and leukocytes sedimented on top of the erythrocyte cushion were resuspended with an equivalent volume of divalent cation-free Hepes/Tyrode buffer ( $17 \text{ mM}$  Hepes [N-2-hydroxyethylpiperazine-N'-2-ethanesulfonic acid],  $130 \text{ mM}$  NaCl,  $2.7 \text{ mM}$  KCl,  $0.4 \text{ mM}$   $\text{NaH}_2\text{PO}_4$ , and  $2.8 \text{ mM}$  dextrose), pH6.5, containing PPACK ( $46 \mu\text{M}$ ), PG  $\text{E}_1$  ( $14 \mu\text{M}$ ), and a reduced amount of apyrase ( $0.65 \text{ ATPase U/ml}$ ). The gently mixed cell suspension was centrifuged twice with the supernatant fluid removed and replaced by a fresh aliquot of Hepes/Tyrode buffer, containing PG  $\text{E}_1$  ( $14 \mu\text{M}$ ) and a reduced amount of apyrase ( $0.325 \text{ ATPase U/ml}$ ), respectively. To adjust platelet count and hematocrit to physiological levels ( $180,000 - 390,000/\mu\text{l}$  and  $38\% - 43\%$ , respectively), the cell fraction was resuspended in Hepes/Tyrode buffer, pH7.4, containing  $50 \text{ mg/ml}$  bovine serum albumin (BSA; Sigma-Aldrich Chemie).

A recombinant VWF drug candidate (rVWF) currently in clinical development [3–5] which contains ultralarge VWF multimers (/+ UL) and a preparation of rVWF derived thereof by chromatographic depletion of ultralarge multimers (-UL) were used (Fig. 1E; friendly gift of Baxter Innovations GmbH, Vienna, Austria). Both preparations were described in detail by Turecek et al. [5] VWF in normal plasma concentration (rVWF, final concentration  $1 \text{ VWF:Ag U/ml}$  Hepes/Tyrode buffer) in physiological salt buffer, neutral pH, and low non-ionic detergent was added to the final cell suspension. For visualization the experiments were performed with a previously fluorescence-labeled rVWF (final concentration  $1 \text{ VWF:Ag U/ml}$  Hepes/Tyrode buffer). To clarify the effect of the VWF cleaving enzyme during flow conditions a recombinant ADAMTS13 solution (rADAMTS13, final concentration  $1 \text{ U/ml}$  Hepes/Tyrode buffer; friendly gift of Baxter Innovations GmbH, Vienna, Austria) in physiological salt buffer, neutral pH, and low non-ionic detergent was added to the flowing blood cell solution. Before the perfusion experiment solutions of magnesium chloride ( $\text{MgCl}_2$ , final concentration  $0.3 \text{ mM}$ ) and calcium chloride ( $\text{CaCl}_2$ , final concentration  $0.6 \text{ mM}$ ) were added to the fluid. Control experiments were performed with whole blood, i.e. no washing, and EDTA, PPACK, PG  $\text{E}_1$ , apyrase added.

### Fluorescence-Labeling of the rVWF

The fluorescence protein labeling of the rVWF was performed with the Alexa Fluor® 488 Labeling Kit (Life Technologies GmbH, Darmstadt). One milliliter protein solution plus  $100 \mu\text{l}$  of a  $1 \text{ M}$  sodium bicarbonate solution were incubated for two hours at room temperature with the Alexa Fluor® 488 dye while constantly stirred in the dark. The free dye was removed from the protein conjugates by extensive dialysis at  $4^\circ\text{C}$  with Slider-A-Lyzer® Mini Dialysis Units (Thermo Fisher Scientific Inc., Rockford, IL) and phosphate buffered saline (PBS) containing sodium azide ( $13 \text{ mg/l}$ ; Sigma-Aldrich). For four days the dialysis buffer was refreshed thrice a day before the protein conjugates were stored in opaque tubes at  $4^\circ\text{C}$ . During the labeling process half the active protein was lost without a change in the multimer distribution (Fig. 1E). The in the experiments used rVWF concentration was adjusted respectively.

### Fluorescence-Labeling of Platelets

In order to fluorescence-label platelets the buffy coat was transferred into another reaction tube after the last blood washing centrifugation step. Per milliliter cell suspension  $1.5 \mu\text{l}$  calcein red-orange AM solution ( $10 \mu\text{g}$  calcein/ $\mu\text{l}$  DMSO; Life Technologies GmbH) were added. After one hour incubation in the dark the buffy coat containing labeled platelets was resuspended in the red blood cell solution and processed as described above.

### Preparation of Perfused Surfaces and In Vitro Perfusion Experiments

Multimeric rVWF with and without ultralarge multimers (coating concentration  $1 \text{ VWF:Ag U/ml}$  Hepes/Tyrode buffer; friendly gift from Baxter Innovations, Vienna) [6] or fibrillar collagen type I (coating concentration  $100 \mu\text{g}$  collagen fibrils/ml buffer; Horm-Chemie; Nycomed, Munich) [7] were coated as substrates onto glass coverslips that were assembled into a parallel plate rectangular flow chamber (height:  $127 \mu\text{m}$ , width:  $2.5 \text{ mm}$ , length:  $25 \text{ mm}$ ). Coating procedures were performed for one hour at room temperature in a wet chamber. Perfusion experiments were conducted at  $37^\circ\text{C}$ . For real-time visualization of platelet-VWF-interactions under high shear rates the flow chamber was mounted on the stage of an upright microscope (Axioskop 2 plus, Carl Zeiss, Jena). With a REGLO Digital MS-2/6 peristaltic pump (IDEX Health & Science GmbH, Glattingen) an artificial blood circulation was established, whereby the chamber was perfused at the desired flow rate (wall shear rates ranging from  $10,000 \text{ s}^{-1}$  up to  $50,000 \text{ s}^{-1}$ ). Platelets and aggregates were observed in bright field illumination ( $100 \text{ W}$  halogen lamp) and the labeled rVWF multimers and nets were observed by epifluorescence microscopy with a HBO-50 AC mercury lamp and a FITC filter block.

A second flow device with a radial stagnation point flow chamber was used to examine the dependence of changed hemodynamics on VWF-platelet interaction [8,9]. Glass coverslips coated as described above were placed in the flow chamber where the surface was perfused by a perpendicular incoming flow (inlet diameter:  $650 \mu\text{m}$ , chamber height:  $480 \mu\text{m}$ ) that symmetrically radiated apart. In the outward regions of the chamber the fluid was collected in a ring channel and pumped off through the outlet. Washed blood cell suspensions containing rVWF/+ UL with labeled platelets was likewise perfused over an rVWF/+ UL or collagen type I coated surface.

### Image Acquisition, Analysis and Statistics

All experiments were recorded live on double sided DVD-RAM/R with a Panasonic LQ-MD800 DVD video recorder at an acquisition rate of 25 frames per second. The images were acquired with a 2/3"-1-CCD-camera (AVT BC-71; Horn Imaging, Aalen) and an optical  $0.33\times - 1.6\times$  zoom. The objective used was a Plan-Neofluar  $40\times/1.30 \text{ NA oil}$  (Carl Zeiss, Ulm). Image analysis was performed offline with the Metamorph software package 6.1 (Molecular Devices). Along the middle axis of an aggregate

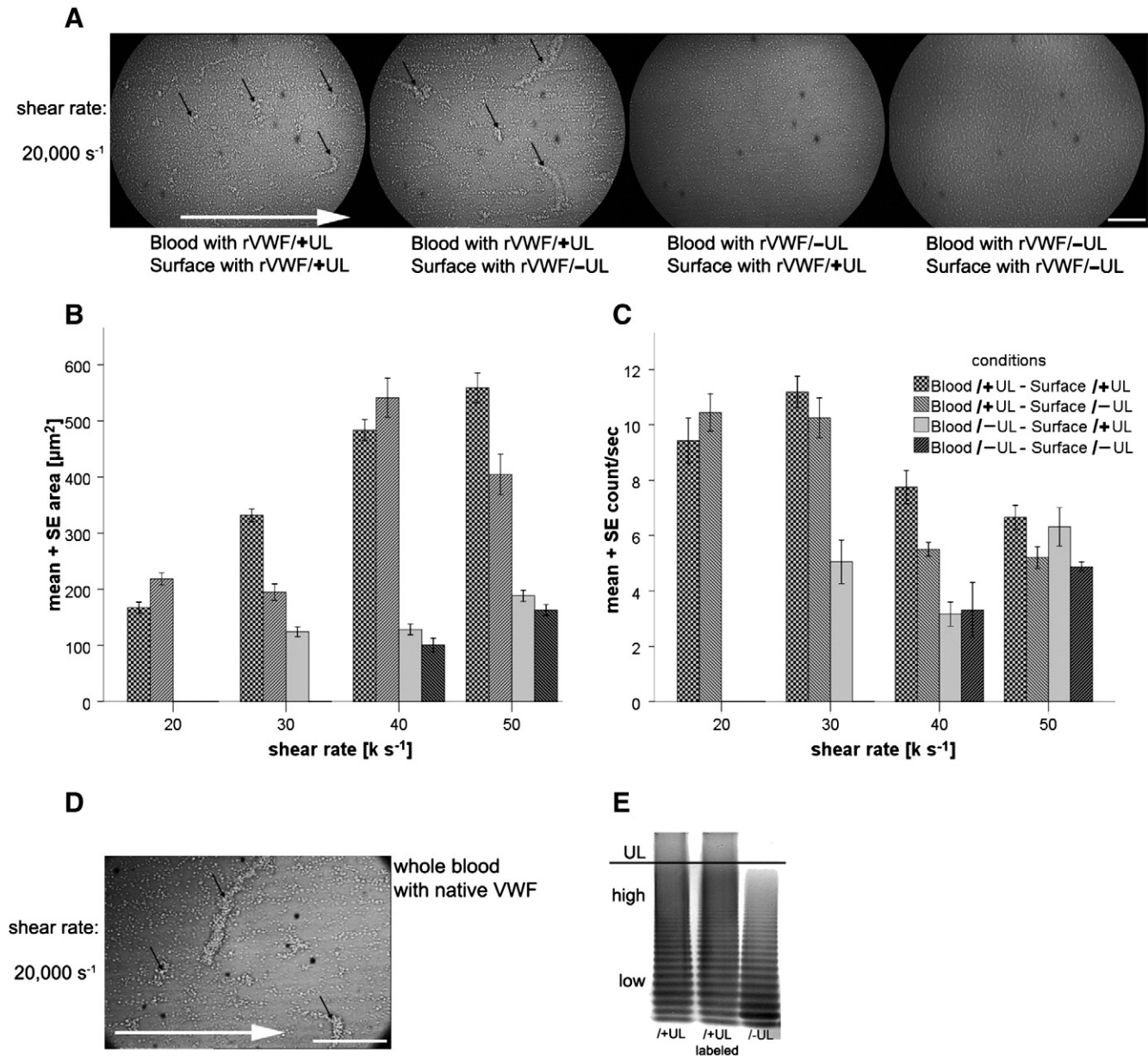


**Fig. 1.** Rolling aggregate formation in washed blood flowing over rVWF coated surface (bright field). Perfusion ( $N = 3$  for each condition) was performed at high shear rates (20,000 s<sup>-1</sup> to 50,000 s<sup>-1</sup>) with washed blood cells suspended in Hepes/Tyrod buffer (pH 7.4) over immobilized rVWF either with (rVWF/+UL) or without (rVWF/-UL) ultralarge VWF molecules (20 μg/mL coating concentration); the buffer solution also contained soluble rVWF with or without ultralarge VWF molecules, respectively. (A) Video-microscopy still images taken at shear rate of 20,000 s<sup>-1</sup> of aggregates (black arrows) formed by activation blocked platelets rolling over the rVWF-coated surface (see also Suppl. Video 1a). Blood containing rVWF/+UL accumulated larger and more aggregates, while blood lacking those (rVWF/-UL) – either in the fluid or on the surface – hardly showed any rolling aggregates. White arrow indicates flow direction. The bar represents 50 μm. (B) Graph shows the surface area (μm<sup>2</sup>) covered by rolling aggregates (mean + se) for shear rates of 20ks<sup>-1</sup>, 30ks<sup>-1</sup>, 40ks<sup>-1</sup> and 50ks<sup>-1</sup>. Higher shear rates resulted in increased coverage and larger rolling aggregates. rVWF/-UL only led to aggregate formation at shear rates above 30ks<sup>-1</sup>. (C) Overall aggregate count appeared to be inversely related to shear rates of 20ks<sup>-1</sup>, 30ks<sup>-1</sup>, 40ks<sup>-1</sup> and 50ks<sup>-1</sup>. (D) Video-microscopy still image taken at shear rate of 20,000 s<sup>-1</sup> of aggregates (black arrows) formed by platelets in citrate anticoagulated whole blood rolling over the rVWF-coated surface (see also Suppl. Video 1a). White arrow indicates flow direction. The bar represents 50 μm. Every experiment was performed for four minutes and 500 (area) or 100 (count) single frames were analyzed respectively. (E) Multimer analysis comparing all used rVWF fractions (friendly provided by Baxter Innovations, Vienna). Molecular weight decreases from top to bottom. The black line borders the ultra large multimers (lacking in the right lane).

their length was measured from tip to tip with a linear dimension tool and their area was analyzed by enclosing them with a polygon tool. Adherent fibers were measured with a linear dimension tool and counted as two when they did not touch each other. Measurements were taken at a distance from the margin of the flow channel of at least 150 μm in parallel flow or within a radial distance around the center of the stagnation point of 300 μm. Every experiment ( $n = 3$ ) was performed for four minutes and single frames were analyzed respectively. For statistical analysis the mean and standard error (SE) were calculated with SPSS17 Statistics 17.0 (IBM, Armonk, NY). If necessary differences between experiments were evaluated with the Mann-Whitney-U-Test. For image

editing Adobe Photoshop Pro CS3 (Adobe Systems Inc., San Jose, CA) was used. The supplemental movies available online were created with Adobe Premiere Pro CS3 (Adobe Systems Inc.).

## Results

### Dependency of Rolling Aggregate Formation on Ultralarge VWF Multimers in Solution and on the Surface

The activation independent but reversible formation of large, mobile platelet aggregates under elevated shear stress was previously shown



(Suppl. Video 1) [1]. Prerequisite for the formation of those aggregates was the presence of both soluble VWF in the fluid and VWF immobilized on the surface. To show their relation with shear rate and platelet aggregate size and count, rVWF preparations were examined that contained all VWF multimer bands but only differed in ultralarge VWF multimer content, i.e. with (VWF/+ UL) and without (rVWF/-UL). Presence of VWF/+ UL resulted in larger rolling aggregates that formed at lower shear rates than with a fluid lacking ultralarge VWF multimers. Therefore the presence of rVWF/+ UL in the fluid seemed to be more important for rolling aggregate formation than rVWF/+ UL on the surface. The greatest effect was seen with rVWF/+ UL both in the fluid and simultaneously coated on the surface. At shear rates lower than  $10,000\text{ s}^{-1}$  only single platelets rolled over the surface and the outcome of elevating the shear rate from  $20,000\text{ s}^{-1}$  to  $50,000\text{ s}^{-1}$  was an increase in aggregate size (Fig. 1A,B; Suppl. Video 1a). With rVWF/+ UL both in the blood and coated on the surface the aggregate size (measured as mean area of the aggregates) rose constantly with increasing shear rate. This was less pronounced with rVWF/+ UL only in suspension and rVWF/-UL on the surface. When no UL VWF was present in the fluid but merely coated on the surface the first small aggregates were only detectable at  $30,000\text{ s}^{-1}$ . With complete lack of rVWF/+ UL initial aggregation started only at  $40,000\text{ s}^{-1}$ . In the latter two conditions only a slight additional size increase was detectable at  $50,000\text{ s}^{-1}$ .

When assessing aggregate count per second (Fig. 1C) the surface-bound rVWF appeared to be of more impact at  $50,000\text{ s}^{-1}$ . Overall the highest aggregate counts were found with rVWF/+ UL in both fluid and surface at  $30,000\text{ s}^{-1}$  and decreasing at higher shear rates. In control experiments with citrate anticoagulated whole blood- with and without activation-blocked platelets (Fig. 1D; Suppl. Video 1aa)- only the natural plasma VWF was in the fluid to interact with platelets. Here the shear dependent appearance of rolling aggregates was qualitative similar to experiments with washed blood cell suspension and rVWF/+ UL.

#### Visualization of rVWF Networks and VWF-Platelet Conglomerates Under High Shear Conditions

To verify the role of VWF molecules in the formation of rolling platelet aggregates rVWF/+ UL molecules were fluorescence-labeled (Alexa Fluor® 488). The fluorescence signal of a single labeled molecule was too weak to be detected. However when VWF self-assembled at higher shear rates as described above, fibers and networks could be detected either rolling over the surface or immobilized on the surface (Fig. 2A; Suppl. Videos 2 and 2a). VWF-networks and platelet aggregates were co-localized in conglomerates as detected with double illumination (bright field + fluorescence; Fig. 2). With rising shear rates the rolling VWF networks steadily increased in length (data shown for  $30,000\text{ s}^{-1}$  and  $40,000\text{ s}^{-1}$ ; Fig. 2B), but were completely reversible below the threshold of  $10,000\text{ s}^{-1}$ . Fig. 2C shows the frequency shift of the network length distribution. For both shear rates the main frequency range of the VWF network length was between 10 and  $70\text{ }\mu\text{m}$ , possibly indicating an optimum net length. Longer networks arose but then disassembled within seconds. The shift of the peak frequency from  $30\text{ }\mu\text{m}$  VWF net length at  $30,000\text{ s}^{-1}$  to  $55\text{ }\mu\text{m}$  length at  $40,000\text{ s}^{-1}$  is suggestive of higher binding forces between the VWF molecules as well as VWF and platelets at higher shear forces.

#### Immobilization of VWF-Platelet Conglomerates on Collagen Type I Coated Surfaces at High Shear

Fluorescence-labeled rVWF molecules adhered from the fluid onto the coated collagen type I fibers and self-assembled to microscopically visible long strands oriented parallel to the flow streamlines. On top of these initial strands large rVWF-networks formed that caught platelets from the flow and accumulated them to large surface bound aggregates (Fig. 3A; Suppl. Video 3). These stable rVWF-platelet conglomerates were either oriented in the flow direction or perpendicular to it in

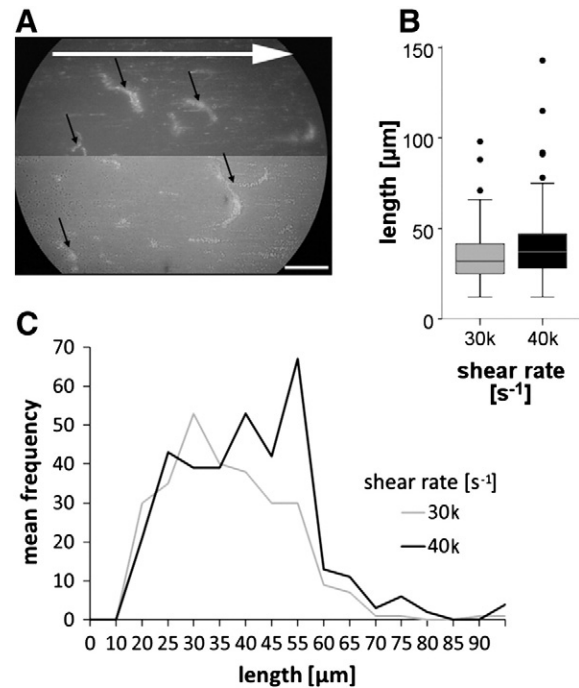


**Fig. 2.** Formation of rolling VWF network/platelet aggregate conglomerate in washed blood containing fluorescence-labeled rVWF with ultra large molecules (rVWF/+ UL). Perfusion ( $N = 3$  for each condition) was performed at high shear rates of  $30,000\text{ s}^{-1}$  and  $40,000\text{ s}^{-1}$  with washed blood cells suspended in Hepes/Tyrode buffer (pH 7.4) containing rVWF/+ UL over immobilized rVWF/+ UL ( $20\text{ }\mu\text{g/mL}$  coating concentration). (A) Video still image of rVWF networks (top) and platelet aggregates (bottom) rolling at  $40,000\text{ s}^{-1}$  over the rVWF surface (see also Suppl. Video 2). The fluorescence-labeled rVWF formed nets co-localizing with the rolling platelet aggregates as depicted with double illumination (bright field and fluorescence); white arrow indicates flow direction. The bar represents  $50\text{ }\mu\text{m}$ . (B) The box plot shows a trend towards increasing length of the network-aggregate conglomerates with higher shear rate  $40,000\text{ s}^{-1}$  with (C) a peak in length at  $55\text{ }\mu\text{m}$  versus  $25\text{ }\mu\text{m}$  for  $40,000\text{ s}^{-1}$  versus  $30,000\text{ s}^{-1}$ , respectively. Every experiment was performed for four minutes and 500 single frames were analyzed respectively.

half-moon forms. As seen with VWF coated surfaces, mobile aggregates rolled over those stable conglomerates but not over the collagen surface itself. Recently Colace and Diamond [10] visualized similar VWF network formation adherent to collagen under high shear whole blood flow. Beyond that we demonstrate in our present study the essential role of ultralarge VWF multimers and their mutual interaction with platelets. The experiments by Colace and Diamond also corroborate our own findings that only VWF and platelets together can create those huge, shear resistant conglomerates.

Comparing the effect of rVWF/+ UL presence and absence (rVWF/-UL) in the fluid showed significant differences (Fig. 3B and C). The length of the VWF strands as well as the size of the attached platelet aggregates doubled when ultra large VWF multimers were present. In experiments lacking ultra large multimers the collagen surface was covered with more but smaller rVWF-strands that hardly bound platelets from the flow (Fig. 3D) suggesting that ultra large multimers were needed in the initial attachment and growth phase.

#### ADAMTS13-Regulating Effect on VWF Self-Assembly Under High Shear Conditions

Within seconds after flow start at a shear rate of  $40,000\text{ s}^{-1}$  labeled rVWF-networks rolled over the VWF coated surface. When rADAMTS13 was added to the fluid at the beginning already after 1 min of flow a diminishing effect was detectable (Fig. 4A; Suppl. Video 4). It led to complete disappearance of VWF-networks at 8–9 minutes of flow (Fig. 4B to D). The normal distribution ( $10\text{--}90\text{ }\mu\text{m}$ ) of the network lengths became positively skewed and ended in a small peak between

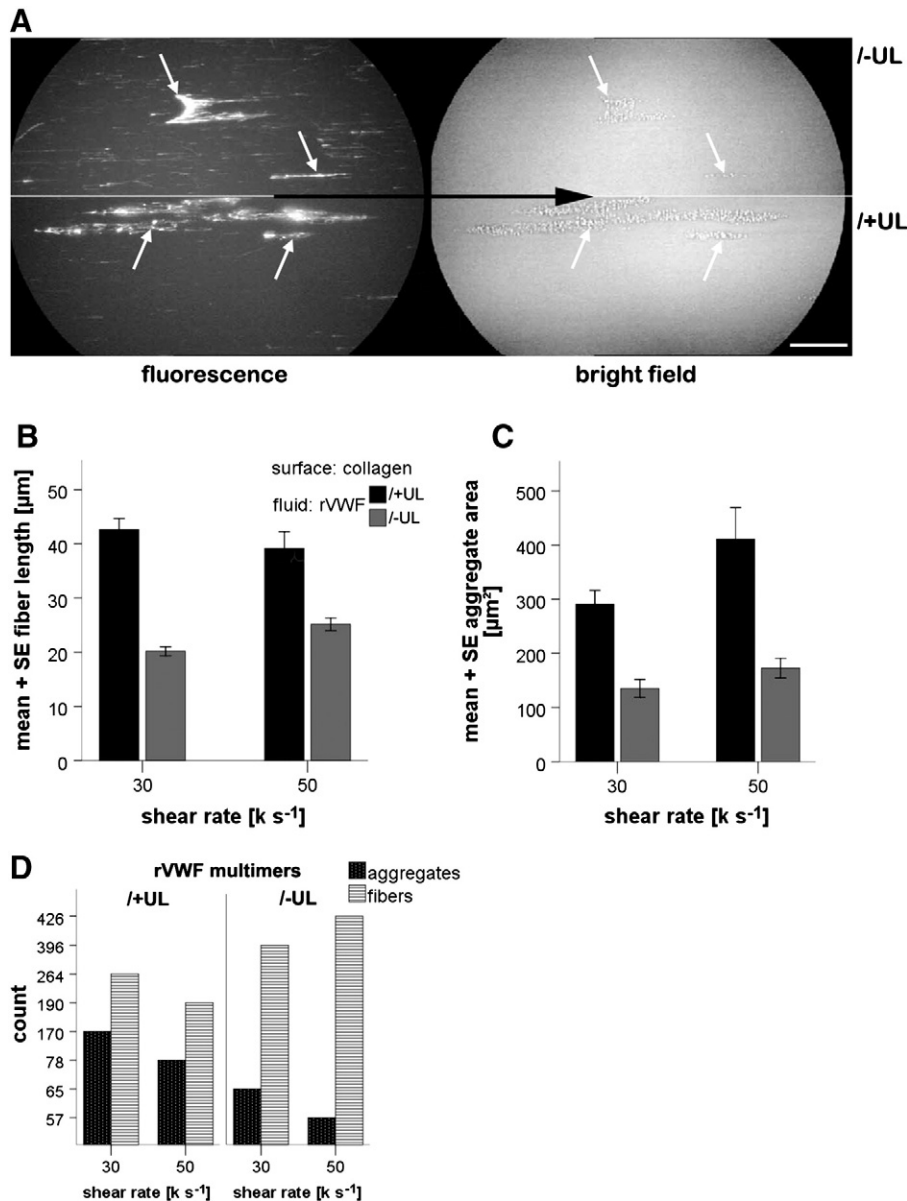


**Fig. 3.** Formation of immobilized and rolling VWF net/platelet aggregate conglomerates on collagen type I surfaces. Perfusion ( $N = 3$  for each condition) over immobilized fibrillar collagen type I was performed at high shear rates of  $30,000 \text{ s}^{-1}$  and  $50,000 \text{ s}^{-1}$  with washed blood cells suspended in Hepes/Tyrosine buffer (pH 7.4) containing fluorescence-labeled rVWF (rVWF/+UL and rVWF/-UL). (A) Video-microscopy still images taken after 3 min flow of adherent rVWF nets (left) and platelet aggregates (right) forming on the collagen surface (see also Suppl. Video 3). rVWF networks co-localized with platelet aggregates as depicted with double illumination (bright field and fluorescence; white arrows). In experiments with cell suspension containing ultra large multimers (bottom panel of A) thicker networks and aggregates formed than without ultra large multimers (top). Furthermore many short rVWF fibers attached to the collagen surface without accumulating platelets from the cell suspension depleted of ultra large multimers (top). Black arrow indicates flow direction (shear rate:  $50,000 \text{ s}^{-1}$ ) and the bar represents  $50 \mu\text{m}$ . (B) The bar graphs show the relation of rVWF fiber length (measured in fluorescence images) and (C) of the area size of platelet aggregates (measured in bright field images) with the presence of ultra large rVWF multimers. (D) depicts the mean count of fibers and aggregates depending on shear rate and rVWF/+UL presence. Every experiment was performed for four minutes and 5 positions within the flow channel were analyzed respectively. The differences between +UL and -UL experiments were significant ( $p < 0.05$ ; Mann-Whitney-U-Test).

10 and  $20 \mu\text{m}$ , before they diminished completely (Fig. 4D). Accordingly surface-adherent rVWF-strands were reduced and had disappeared after 15 minutes (Fig. 4E). These results demonstrate rADAMTS13 as effective regulatory counterpart to the highly reactive ultralarge rVWF.

#### Dependency of Platelet-VWF Interactions on Hemodynamics

In order to expand our study beyond wall parallel flow we examined VWF-platelet interaction and conglomerate formation in stagnation point flow, a complex flow condition present in vessel bifurcations and curvatures as well as downstream of severe stenosis. Stagnation point flow has a flow component directed perpendicular to the

wall. Thus a wall shear gradient is generated that is zero in the center, has a peak at a distance ( $241 \mu\text{m}$ ) and decreases again further outwards. In spite of principal hemodynamic differences between both flow conditions we observed the same phenomenon of rolling aggregates as with wall parallel flow using rVWF/+UL in the fluid and coated on the surface (Fig. 5A; Suppl. Video 5). With increasing peak shear rates the average aggregate length steadily augmented (Fig. 5B). However in stagnation point flow rolling platelet aggregates were already detectable at a peak shear rate of  $8,000 \text{ s}^{-1}$  compared to wall parallel flow (cf. Fig. 2), indicating a positive influence onto platelet-VWF interactions through the flow situation. Details to the flow field and shear rate profile are shown in Fig. 5C.

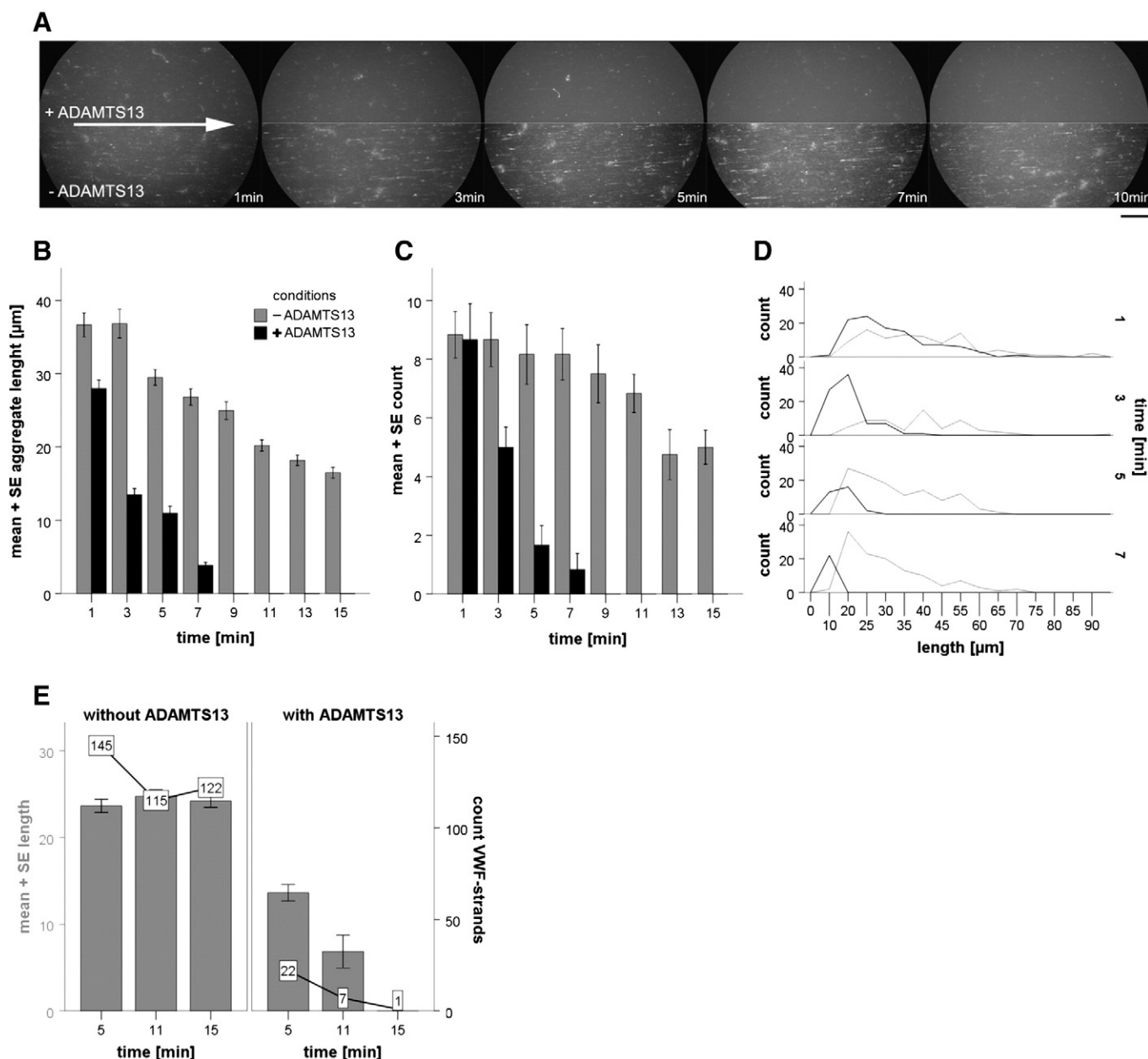


**Fig. 4.** Kinetics of rADAMTS13 effect on rVWF network formation under high shear rates. Perfusion ( $N = 3$ ) was performed over immobilized rVWF/+UL at a shear rate of  $40,000 \text{ s}^{-1}$  with a washed blood cell suspension containing fluorescence labeled rVWF. (A) Video-microscopy still images taken after certain time points illustrating the formation and degradation of rVWF-networks (see also Suppl. Video 4). Experiments with rADAMTS13 (top; 1 Unit/ml) were compared to a control without rADAMTS13 (bottom) over a period of 10 minutes flow. Arrow indicates flow direction. The bar represents  $50 \mu\text{m}$ . (B) The diminishing and finally abolishing effect of rADAMTS13 on VWF fiber length as well as (C) the count of rolling conglomerates is shown in the bar graphs. (D) The first 7 minute period was analyzed for the length distribution of the conglomerates. Starting with a similar distribution with + rADAMTS13 (black line) and without -rADAMTS13 (grey line), the presence of ADAMTS13 led to a narrow peak of VWF net length at around  $10 \mu\text{m}$ , while absence of ADAMTS13 maintained a wide length distribution up to  $75 \mu\text{m}$ . (E) Similar results as shown in (B) and (C) for rolling conglomerates are depicted for rVWF fibers attached to the surface. The diminishing effect of ADAMTS13 on VWF in length (bar graph) and count (line graph) is determined after 15 minutes of flow. For every time step in the experiments 3 positions within the flow channel were analyzed respectively.

## Discussion

Homotypic self-association of soluble VWF with surface immobilized VWF has been reported to occur at shear rate  $1,500 \text{ s}^{-1}$  [11]. Our current experiments provide the first direct visual evidence of VWF molecules self-assembly in flow as well as on the surface at shear rates of  $20,000 \text{ s}^{-1}$  and above. Platelets, which were incorporated in the VWF strands network - were at the same time a prerequisite as well as a stabilizer for the platelet-VWF conglomerates. That such polymer-colloid composite assembly in shear flow seems to be a universal process was reported recently [2]. In the present study we went further and examined the self-

assembly of the polymer, i.e. VWF: our real-time visualization demonstrated the formation of VWF strands and networks that were up to  $10 \mu\text{m}$  in diameter and up to  $100 \mu\text{m}$  in length, thus requiring VWF self-assembly in order to reach such dimensions clearly above single molecule size. The VWF-platelet structures were not only resisting the high shear stress but actually fostered by it, suggesting catch bonds between the platelet GPIb receptor and the VWF A1 domain [12]. There seems to be the indication that strong intermolecular cysteine bonds [13] could favor the interaction between single VWF molecules and high shear rates activate the VWF molecule by uncoiling it [14,15].



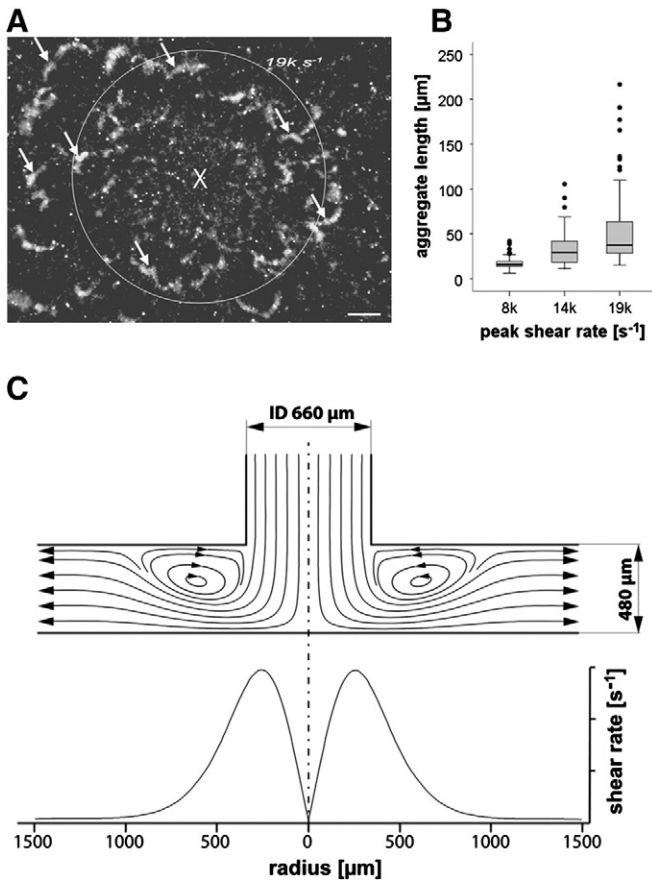


**Fig. 5.** Rolling aggregate formation in a stagnation point flow in the presence of rVWF/+UL. Perfusion ( $N = 3$ ) with washed blood cells suspended in Hepes/Tyrosine buffer started at peak shear rates of  $3,500 s^{-1}$  and was increased up to  $19,000 s^{-1}$ . VWF containing rVWF/+UL was in the fluid and coated on the cover slips ( $20 \mu g/mL$  coating concentration). The flow was directed perpendicular to the surface and radiated rotationally symmetrical. (A) Video-microscopy still image depicting the larger platelet aggregates (white arrows) at a distance to the stagnation point (white X) where the peak shear rate of  $19k s^{-1}$  occurs (white circle; distance to X:  $241 \mu m$ ) (see also Suppl. Video 5). Rolling aggregates were growing until reaching the peak shear rate and diminished further outward with decreasing shear rate. The bar represents  $50 \mu m$ . (B) The box plot shows increasing length of platelet aggregates with higher shear rate but already starting at a threshold approximately half the shear rate as observed in wall parallel flow. (C) The illustration (above) depicts the flow field in the stagnation point flow chamber at high shear rates. The chamber is rotationally symmetric as described by Affeld et al. The characteristic wall shear rate profile at the lower wall (below) is plotted as a function of the radial distance from the center of stagnation point [9] (Kindly provided by J. Schaller from the Biofluid Mechanics Laboratory, Charité Berlin). Every experiment was performed for one minute for each velocity and 3 single frames representing the complete area around the stagnation point were analyzed respectively.

At the beginning a single platelet rolling over a VWF coated surface and interacting via its GPIIb/IIIa receptor with the A1-domain of the immobilized VWF can at the same time interact with soluble VWF flowing in the adjacent fluid layer. If the shear rate exceeds a critical threshold the previously globular, i.e. coiled, VWF molecule can be stretched via the shear force [2,15]. Then it can capture more platelets via the A1-domain exposed on the stretched molecule. In a self-amplifying manner platelets attached to the elongated VWF molecule can act in a sail like fashion to increase the stretching of the molecule thus exposing more A1-domain. In turn more A1-domain can bind to more GPIIb/IIIa receptors either on the same platelet or on newly captured ones. On the surface of those platelets more VWF can bind with a repetition of the above sequence of steps. Thereby single molecule strands would bind to platelet surfaces and act as glue between non-activated platelets. In addition a shear dependent VWF self-assembly mechanism between the individual VWF molecules appears to be present, the biochemistry of which we have not yet analyzed further (Fig. 6). This

process was demonstrated before with experiments by Steppich et al. [16] and Savage et al. [11].

Still in its ultralarge form the von Willebrand Factor multimer is released from its endothelial Weibel-Palade storage sites upon endothelial activation due to adjacent vessel injury or inflammation [17–19] and gives a better halt for VWF-platelet conglomerates. After its exposure to its cleaving enzyme ADAMTS13 that resides in the plasma, VWF is broken down into a multimer pattern of varying sizes lacking the ultralarge multimers or even large multimers when high shear forces persist [20]. In our experiments we detected a hitherto unrecognized role for the ultralarge VWF molecules: formation of rolling platelet aggregates was markedly enhanced in the presence of rVWF/+UL when compared to preparations lacking only the ultralarge rVWF portion, but with all other multimers present. Platelet-VWF string formation was described for low shear flow conditions over inflammation stimulated endothelium that therefore released UL-VWF [17–19]. Ultralarge rVWF multimers seem to be “stickier” than rVWF lacking UL as indicated by others [21] and assessed by the increased capture of platelets that gradually augmented with elevated shear rates thereby forming larger aggregates in our experiments. VWF activity has been attributed to shear forces causing a conformational change in VWF from globular to elongated shape [2,14,15]. In its globular state the A1A2A3 domains of each monomer form intramolecular bonds that are broken by elevated shear forces, thus potentially allowing interaction with bonding partners on other molecules or receptors [22,23]. Thus, with elevating shear rates more and more intermolecular interactions could stabilize VWF-VWF bonds as well as larger platelet aggregates incorporated into such VWF networks rolling over the surface. This would represent an improvement in efficiency of VWF binding and platelet accrual due to elevated shear forces.

At a certain shear threshold, when enough platelet binding VWF-A1 domains as well as the hypothetical VWF-VWF bonding sites are exposed, VWF self-assembly as well as aggregation of non-activated platelets could start. Saturation would be a condition when all binding sites are occupied by platelets and the shear stress exceeds the force of intermolecular cohesions and this may lie well beyond  $100,000 s^{-1}$  [24]. Different reactivity patterns between rVWF/+UL and rVWF/-UL may come from the analysis of pre-activation of ultralarge VWF multimers [25,26]. The tensile force on a VWF multimer increases with the square of multimer length and is highest in the middle of the molecule; in addition cleaved VWF is activated by arterial shear forces whereas uncleaved VWF, i.e. containing ultralarge multimers, is activated at lower shear stresses [25]. A positive feedback loop could be envisioned where this mechanism is operational for strings and even networks of assembled VWF multimers at shear rates of  $20,000 s^{-1}$  and above. The massive amount of rolling aggregates in the control experiments with whole blood (not washed) suggests at least the presence of trace amounts of UL molecules in whole blood, not detectable with our methods.

Under high shear flow platelets initially arrest on collagen fibers via VWF, i.e. VWF binds to collagen [10,27] via its A3 domain and exposes its A1-domain to the platelet GPIIb/IIIa receptor. Our results suggest that more VWF is bound to collagen in the presence of ultralarge VWF molecules in solution and that subsequently more platelets deposit. Since soluble rVWF can bind to GPIIb/IIIa on the apical surface of adherent platelets a new VWF surface is presented to the next platelets flowing by in adjacent fluid layers. We observed growth in size of rolling aggregates and platelet-VWF conglomerates with increasing shear rates but also that aggregates rolled over the apical surface of platelet aggregates already immobilized on collagen in the experiments where rVWF/+UL was present. Our finding takes previous reports for an in vivo mouse model and an in vitro human whole blood model further by specifying and directly visualizing the role of ultralarge VWF multimers [1,10].

The only enzyme counteracting the thrombogenic effect of VWF is the metalloprotease ADAMTS13, which degrades VWF multimers under elevated shear stress [28] by high affinity binding to VWF and

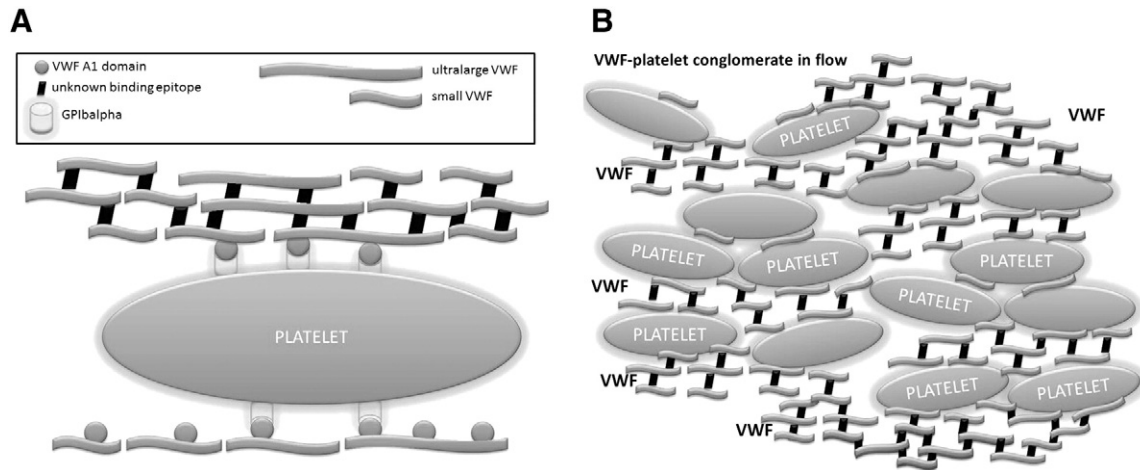


**Fig. 6.** Schematic concept of initial platelet adhesion and VWF-platelet conglomerate formation. (A) Once von Willebrand factor is immobilized from the solution onto the surface its A1 domains will capture and arrest platelets via their GPIIb/IIIa-receptors. Adherent platelets will attract more VWF on their luminal side, again via GPIIb/IIIa-receptors. Due to the shear activation of VWF its self-assembly can be hypothesized on such platelet layers. (B) Rolling VWF-platelet conglomerates can form under very high shear conditions with mutual reinforcement and again based on the hypothetical VWF self-assembly.

cleaving the shear-unfolded A2-domain. Binding sites for ADAMTS13 on the globular VWF multimer associates both molecules during normal flow conditions and thus preventing unwanted platelet aggregation by fast cleavage in case of unfolding [29]. In normal hemostasis VWF secreted from endothelial cells has been reported to be completely degraded by ADAMTS13 within two hours [25,30]. Under pathological conditions of i.e. aortic stenosis or left ventricular assist devices decreased large VWF levels indicate a higher ADAMTS13 activity due to elevated shear [31,32]. Our own findings show that the indicator for the explicit role of the rVWF/+ UL under high shear flow, i.e. the platelet-VWF conglomerates and rolling aggregates – disappear within minutes in the presence of ADAMTS13. Hassan et al. [30] showed that the exposure time to high shear rates is secondary to the magnitude of it. In addition we show that surface-attached VWF strands last at least two-fold longer than in solution, which would be a beneficial feature in the scenario of wound closure after vessel injury. If platelet aggregates that are deposited via a VWF mesh on a surface are still affected by ADAMTS13 activity still remains to be answered.

For more than 120 years disturbed hemodynamics have been reported to have large influence on hemostasis and thrombosis [33–35]. In particular not only shear in wall-parallel flow, but other flow components, e.g. present in stagnation point, flow appeared to have substantial influence on platelet aggregation as well as fibrin clot formation [8,36–39]. Further experimental evidence is needed to clarify the interaction of the various forces in play.

Here we demonstrate that von Willebrand factor can reversibly self-assemble in flowing blood exhibiting extremely high shear rates and can be down-regulated by ADAMTS13 within minutes. The accrual of large platelet masses by the shear dependent formation of VWF self-assembly and VWF-platelet conglomerate formation may be interpreted as rapid-response system to stop initial wound bleeding even before activation of platelets and the clotting system can take place. In a pathological setting this could accelerate thrombus development occurring in the course of minutes [24,40]. An additional function of these VWF networks may be the protection of platelets against shear induced lysis as found by Anderson and coworkers [41] due to force absorption by the VWF strands. However this still requires further evidence.

Supplementary data to this article can be found online at <http://dx.doi.org/10.1016/j.thromres.2014.03.024>.

#### Authorship Contributions

TK and MN performed and analyzed the experiments; MAF fluorescence-labeled the recombinant von Willebrand factor; HG

analyzed the rVWF multimers; MFS and AJR developed the concept; TK and AJR wrote the manuscript. No conflicts of interest.

#### Acknowledgements

The authors want to thank Hans Peter Rottensteiner, Peter L. Turecek and Friedrich Scheifflinger from Baxter Innovations GmbH, Vienna Austria, for their valuable discussions and comments and for the friendly gift of the recombinant von Willebrand factor preparations as well as recombinant ADAMTS13. They also want to thank Jennifer I. Angerer from the University of Augsburg for her help with the protein labeling and J. Schaller from the Charité Berlin for the CFD simulation of the flow fields. MFS thanks the German Research Foundation (DFG) SHENC – Research Unit FOR1543 for a guest professorship.

#### References

- [1] Ruggeri ZM, Orje JN, Habermann R, Federici AB, Reininger AJ. Activation-independent platelet adhesion and aggregation under elevated shear stress. *Blood* 2006;108:1903–10.
- [2] Chen H, Fallah MA, Huck V, Angerer JI, Reininger AJ, Schneider SW, et al. Blood-clotting-inspired reversible polymer-colloid composite assembly in flow. *Nat Commun* 2013;4:7.
- [3] Mannucci PM, Kempton C, Millar C, Romond E, Shapiro A, Birschmann I, et al. Pharmacokinetics and safety of a novel recombinant human von Willebrand factor manufactured with a plasma-free method: a prospective clinical trial. *Blood* 2013;122:648–57.
- [4] Turecek PL, Mitterer A, Matthiessen HP, Gritsch H, Varadi K, Siekmann J, et al. Development of a plasma- and albumin-free recombinant von Willebrand factor. *Hamostaseologie* 2009;29:32–8.
- [5] Turecek PL, Schrenk G, Rottensteiner H, Varadi K, Bevers E, Lenting P, et al. Structure and Function of a Recombinant von Willebrand Factor Drug Candidate. *Semin Thromb Hemost* 2010;36:510–21.
- [6] Savage B, Saldivar E, Ruggeri ZM. Initiation of platelet adhesion by arrest onto fibrinogen or translocation on von Willebrand factor. *Cell* 1996;84:289–97.
- [7] Savage B, Almus-Jacobs F, Ruggeri ZM. Specific synergy of multiple substrate-receptor interactions in platelet thrombus formation under flow. *Cell* 1998;94:657–66.
- [8] Reininger AJ, Korndorfer MA, Wurzing J. Adhesion of ADP-activated platelets to intact endothelium under Stagnation Point Flow in vitro is mediated by the integrin alpha IIb beta 3. *Thromb Haemost* 1998;79:998–1003.
- [9] Affeld K, Goubergrits L, Kertzscher U, Gadischke J, Reininger A. Mathematical model of platelet deposition under flow conditions. *Int J Artif Organs* 2004;27:699–708.
- [10] Colace TV, Diamond SL. Direct Observation of von Willebrand Factor Elongation and Fiber Formation on Collagen During Acute Whole Blood Exposure to Pathological Flow. *Arterioscler Thromb Vasc Biol* 2013;33:105–13.
- [11] Savage B, Sixma JJ, Ruggeri ZM. Functional self-association of von Willebrand factor during platelet adhesion under flow. *Proc Natl Acad Sci U S A* 2002;99:425–30.
- [12] Yago T, Lou J, Wu T, Yang J, Miner JJ, Coburn L, et al. Platelet glycoprotein Ib alpha forms catch bonds with human WT vWF but not with type 2B von Willebrand disease vWF. *J Clin Invest* 2008;118:3195–207.
- [13] Ganderton T, Wong JWH, Schroeder C, Hogg PJ. Lateral self-association of VWF involves the Cys2431-Cys2453 disulfide/dithiol in the C2 domain. *Blood* 2011;118:5312–8.



- [14] Siedlecki CA, Lestini BJ, KottkeMarchant K, Eppell SJ, Wilson DL, Marchant RE. Shear-dependent changes in the three-dimensional structure of human von Willebrand factor. *Blood* 1996;88:2939–50.
- [15] Schneider SW, Nuschele S, Wixforth A, Gorzelanny C, Alexander-Katz A, Netz RR, et al. Shear-induced unfolding triggers adhesion of von Willebrand factor fibers. *Proc Natl Acad Sci U S A* 2007;104:7899–903.
- [16] Steppich DM, Angerer JI, Sriharan K, Schneider SW, Thalhammer S, Wixforth A, et al. Relaxation of ultralarge VWF bundles in a microfluidic-AFM hybrid reactor. *Biochem Biophys Res Commun* 2008;369:507–12.
- [17] Barg A, Ossig R, Goerge T, Schneider MF, Schillers H, Oberleithner H, et al. Soluble plasma-derived von Willebrand factor assembles to a homeostatically active filamentous network. *Thromb Haemost* 2007;97:514–26.
- [18] Goerge T, Kleinerueschkamp F, Barg A, Schnaeker E-M, Huck V, Schneider MF, et al. Microfluidic reveals generation of platelet-strings on tumor-activated endothelium. *Thromb Haemost* 2007;98:283–6.
- [19] Chauhan AK, Goerge T, Schneider SW, Wagner DD. Formation of platelet strings and microthrombi in the presence of ADAMTS-13 inhibitor does not require P-selectin or beta(3) integrin. *J Thromb Haemost* 2007;5:583–9.
- [20] Sadler JE. Aortic stenosis, von Willebrand factor, and bleeding. *N Engl J Med* 2003;349:323–5.
- [21] Groot E, de Groot PG, Fijnheer R, Lenting PJ. The presence of active von Willebrand factor under various pathological conditions. *Curr Opin Hematol* 2007;14:284–9.
- [22] Auton M, Sowa KE, Behymer M, Cruz MA. N-terminal Flanking Region of A1 Domain in von Willebrand Factor Stabilizes Structure of A1A2A3 Complex and Modulates Platelet Activation under Shear Stress. *J Biochem* 2012;287:14579–85.
- [23] Reininger AJ, Heijnen HFG, Schumann H, Specht HM, Schramm W, Ruggeri ZM. Mechanism of platelet adhesion to von Willebrand factor and microparticle formation under high shear stress. *Blood* 2006;107:3537–45.
- [24] Bark Jr DL, Para AN, Ku DN. Correlation of thrombosis growth rate to pathological wall shear rate during platelet accumulation. *Biotechnol Bioeng* 2012;109:2642–50.
- [25] Zhang X, Halvorsen K, Zhang C-Z, Wong WP, Springer TA. Mechanoenzymatic Cleavage of the Ultralarge Vascular Protein von Willebrand Factor. *Science* 2009;324:1330–4.
- [26] Springer TA. Biology and physics of von Willebrand factor concatamers. *J Thromb Haemost* 2011;9:130–43.
- [27] Westein E, van der Meer AD, Kuijpers MJE, Frimat JP, van den Berg A, Heemskerk JWM. Atherosclerotic geometries exacerbate pathological thrombus formation poststenosis in a von Willebrand factor-dependent manner. *Proc Natl Acad Sci U S A* 2013;110:1357–62.
- [28] McGrath RT, McKinnon TAJ, Byrne B, O'Kennedy R, Terraube V, McRae E, et al. Expression of terminal alpha 2-6-linked sialic acid on von Willebrand factor specifically enhances proteolysis by ADAMTS13. *Blood* 2010;115:2666–73.
- [29] Crawley JTB, de Groot R, Xiang Y, Luken BM, Lane DA. Unraveling the scissile bond: how ADAMTS13 recognizes and cleaves von Willebrand factor. *Blood* 2011;118:3212–21.
- [30] Hassan MI, Saxena A, Ahmad F. Structure and function of von Willebrand factor: the protein that is deficient and/or abnormal in inherited von Willebrand disease. *Blood Coagul Fibrinolysis* 2012;23:11–22.
- [31] Hollestelle MJ, Loots CM, Squizzato A, Renne T, Bouma BJ, de Groot PG, et al. Decreased active von Willebrand factor level owing to shear stress in aortic stenosis patients. *J Thromb Haemost* 2011;9:953–8.
- [32] Meyer AL, Malehsa D, Bara C, Budde U, Slaughter MS, Haverich A, et al. Acquired von Willebrand Syndrome in Patients With an Axial Flow Left Ventricular Assist Device. *Circ Heart Fail* 2010;3:675–81.
- [33] Eberth CJ, Schimmelbusch C. Die Thrombose nach Versuchen und Leichenbefunden. Stuttgart: Verlag von Ferdinand Enke; 1888.
- [34] Karino T, Goldsmith HL, Motomiya M, Mabuchi S, Soharu Y. Flow patterns in vessels of simple and complex geometries. *Ann N Y Acad Sci* 1987;516:422–41.
- [35] Wolberg AS, Aleman MM, Leiderman K, Machlus KR. Procoagulant Activity in Hemostasis and Thrombosis: Virchow's Triad Revisited. *Anesth Analg* 2012;114:275–85.
- [36] Reininger AJ, Reininger CB, Wurzinger LJ. The influence of fluid-dynamics upon adhesion of ADP-stimulated human platelets to endothelial-cells. *Thromb Res* 1993;71:245–9.
- [37] Reininger AJ, Reininger CB, Heinzmann U, Wurzinger LJ. Residence time in niches of stagnant flow determines fibrin clot formation in an arterial branching model - detailed flow-analysis and experimental results. *Thromb Haemost* 1995;74:916–22.
- [38] Nesbitt WS, Westein E, Tovar-Lopez FJ, Tolouei E, Mitchell A, Fu J, et al. A shear gradient-dependent platelet aggregation mechanism drives thrombus formation. *Nat Med* 2009;15:665–73.
- [39] Bajd F, Vidmar J, Fabjan A, Blinc A, Kralj E, Bizjak N, et al. Impact of altered venous hemodynamic conditions on the formation of platelet layers in thromboemboli. *Thromb Res* 2012;129:158–63.
- [40] Reininger AJ, Bernlochner I, Penz SM, Ravanat C, Smethurst P, Farndale RW, et al. A 2-Step Mechanism of Arterial Thrombus Formation Induced by Human Atherosclerotic Plaques. *J Am Coll Cardiol* 2010;55:1147–58.
- [41] Anderson GH, Hellums JD, Moake JL, Alfrey CP. Platelet lysis and aggregation in shear fields. *Blood Cells* 1978;4:499–507.